



# Heterogeneous Flagellar Expression in Single *Salmonella* Cells Promotes Diversity in Antibiotic Tolerance

Zhihui Lyu,<sup>a</sup> Angela Yang,<sup>a</sup> Patricia Villanueva,<sup>a</sup> Abhyudai Singh,<sup>b</sup>  Jiqiang Ling<sup>a</sup>

<sup>a</sup>Department of Cell Biology and Molecular Genetics, The University of Maryland, College Park, Maryland, USA

<sup>b</sup>Department of Electrical and Computer Engineering and Biomedical Engineering, University of Delaware, Newark, Delaware, USA

**ABSTRACT** Phenotypic heterogeneity among single cells in a genetically identical population leads to diverse environmental adaptation. The human and animal pathogen *Salmonella enterica* serovar Typhimurium exhibits heterogeneous expression of virulence genes, including flagellar and *Salmonella* pathogenicity island (SPI) genes. Little is known about how the differential expression of flagellar genes among single cells affects bacterial adaptation to stresses. Here, we have developed a triple-fluorescence reporter to simultaneously monitor the expression of flagellar and SPI-1 pathways. We show that the two pathways cross talk at the single-cell level. Intriguingly, cells expressing flagella (*fliC*-ON) exhibit decreased tolerance to antibiotics compared to *fliC*-OFF cells. Such variation depends on TolC-dependent efflux pumps. We further show that *fliC*-ON cells contain higher intracellular proton concentrations. This suggests that the assembly and rotation of flagella consume the proton motive force and decrease the efflux activity, resulting in antibiotic sensitivity. Such a trade-off between motility and efflux highlights a novel mechanism of antibiotic tolerance.

**IMPORTANCE** Antibiotic resistance and tolerance pose a severe threat to human health. How bacterial pathogens acquire antibiotic tolerance is not clear. Here, we show that the human and animal pathogen *Salmonella* divides its population into subgroups that are different in their abilities to tolerate antibiotic treatments. In a *Salmonella* population that is genetically identical, some cells express flagella to move toward nutrients, while other cells do not express flagella. Interestingly, we show that *Salmonella* cells that do not express flagella are more tolerant to antibiotics. We have further determined the mechanism underlying such diverse responses to antibiotics. Flagellar motility uses cellular energy stored in the form of proton motive force and makes cells less efficient in pumping out toxic molecules such as antibiotics. The overall bacterial population therefore gains benefits from such diversity to quickly adapt to different environmental conditions.

**KEYWORDS** single cell, antibiotic tolerance, flagella, pathogenesis, *Salmonella*

Genetically identical individuals living in the same microenvironment may exhibit different phenotypes. In recent years, such phenotypic heterogeneity has become a major research focus covering studies ranging from the sources of gene expression noise to the resulting functional consequences (1–4). One of the best-known examples of phenotypic heterogeneity is antibiotic tolerance, which allows a subpopulation of bacterial cells to survive transient antibiotic exposure (5, 6). Tolerance has become a significant cause of antibiotic failure in clinics and has been actively targeted to improve the treatment of bacterial infections (7). Furthermore, drug tolerance has been shown to promote the evolution of permanent antibiotic resistance (8, 9), which exacerbates the urgent threat of drug-resistant microbial infections. Antibiotic

**Citation** Lyu Z, Yang A, Villanueva P, Singh A, Ling J. 2021. Heterogeneous flagellar expression in single *Salmonella* cells promotes diversity in antibiotic tolerance. mBio 12: e02374-21. <https://doi.org/10.1128/mBio.02374-21>.

**Editor** Eduardo A. Groisman, Yale School of Medicine

**Copyright** © 2021 Lyu et al. This is an open-access article distributed under the terms of the [Creative Commons Attribution 4.0 International license](https://creativecommons.org/licenses/by/4.0/).

Address correspondence to Jiqiang Ling, [jlj12@umd.edu](mailto:jlj12@umd.edu).

**Received** 9 August 2021

**Accepted** 27 August 2021

**Published** 28 September 2021

tolerance has been mostly associated with slow growth or low metabolism (10–12), although the underlying mechanisms remain elusive.

*Salmonella enterica* serovar Typhimurium is a bacterial pathogen in animals and humans and causes tens of millions of gastrointestinal infections in humans worldwide each year (13–15). In addition to gastroenteritis, *S. Typhimurium* and other nontyphoidal *Salmonella* strains also cause invasive human disease that often leads to death (14). Among the major virulence genes of *S. Typhimurium* are *Salmonella* pathogenicity island (SPI) and flagellar genes (16, 17). SPI-1 and SPI-2 genes are important for invasion of host cells and intracellular survival, respectively (18). Flagella are critical for *Salmonella* to move toward nutrients as well as within the host (19). In addition, the flagellin protein FliC stimulates the host immune response by activating caspase-1 in macrophages (15). The assembly and rotation of flagella both require proton motive force (PMF) and are energetically costly (19, 20). It has been shown that shutting off flagellar expression helps *Salmonella* cells evade the host immune response (21) and improve growth in culture (22). Interestingly, flagellar and SPI-1 expression is heterogeneous in *Salmonella* (23–27). The expressions of flagellar and SPI-1 pathways are interconnected at the population level (28). In this study, we constructed a triple-fluorescence reporter to detect SPI-1 and flagellar expression simultaneously and found that the expression of these two pathways was positively correlated among single *S. Typhimurium* cells. We next applied this reporter to study the functional impact resulting from the heterogeneous expression of flagellar and SPI-1 genes. To our surprise, we found that *fliC*-OFF cells displayed improved tolerance to bactericidal antibiotics compared with *fliC*-ON cells, in a manner independent of SPI-1 genes. We further show that the heterogeneous responses of *fliC*-ON and *fliC*-OFF cells to antibiotics depend on the efflux activity driven by PMF. Our results suggest that the expression and rotation of flagella compete with the efflux process for PMF. This trade-off leads to lower efflux activity and drug tolerance in cells expressing flagellar genes.

## RESULTS

**Cross talk between SPI-1 and flagellar pathways in single *Salmonella* cells.** Our recent study of the role of protein synthesis in *Salmonella* virulence suggests that perturbing translational fidelity results in the downregulation of both SPI-1 and flagellar genes (29), leading us to further investigate the interplay between these two pathways. Previous studies have shown that the expressions of SPI-1 and flagellar genes in *Salmonella* are correlated at the population level (28). To monitor these two pathways concurrently in single cells, we constructed a low-copy-number plasmid carrying three fluorescence proteins. The *mCherry* gene (encoding a red fluorescent protein) is under the control of a constitutive *Ptet* promoter, serving as a reference for the overall gene expression activity in cells; the *YFP* gene (encoding a yellow fluorescent protein) is controlled by the promoter of *prgH*, which is a downstream SPI-1 gene; and the *eCFP* gene (encoding an enhanced cyan fluorescent protein) is fused to the promoter of *fliC*, a class 3 flagellar gene encoding the flagellin, as a reporter for the expression of the flagellar pathway. Using fluorescence microscopy, we observed the bimodal expression of both the *prgH* and *fliC* promoters in wild-type (WT) *S. Typhimurium* ATCC 14028s cells grown in high-salt Luria broth (LB Miller) (Fig. 1A). This was consistent with previous results from single reporters of SPI-1 and flagellar pathways, respectively (24, 25). Further flow cytometry analysis revealed that the expression of *prgH* and *fliC* was indeed positively correlated (Fig. 1B to D; see also Fig. S1 in the supplemental material). The master regulator of SPI-1 genes is HilD, which controls the expression of HilA (28, 30, 31). HilA in turn activates the expression of downstream SPI-1 genes, including *prgH* (Fig. 2A). As expected, deleting *hilD* or *hilA* abolished the expression of the *prgH* promoter, whereas deleting the master flagellar regulator *flhDC* abolished the expression of *PfliC* (Fig. 2B and C). These results confirm that our triple-fluorescence reporter accurately and sensitively measures the expression of both the SPI-1 and flagellar pathways in single cells.

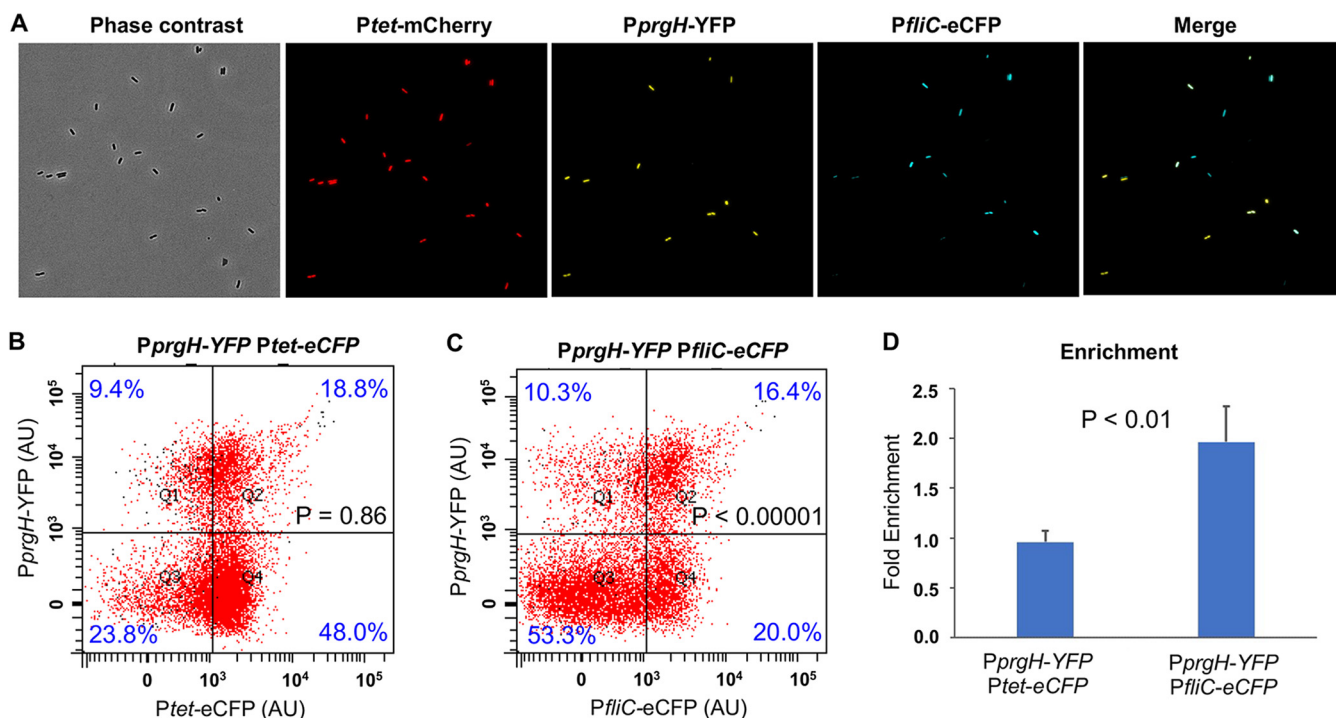


**FIG 1** SPI-1 and flagellar expression are correlated in single *Salmonella* cells. (A) Phase-contrast and fluorescence microscopy of WT *S. Typhimurium* (ATCC 14028s) carrying pZS *Ptet-mCherry PprgH-YFP PfliC-eCFP*. Cells were grown in LB Miller at 37°C for 5 h to the early stationary phase prior to imaging. While the constitutive *Ptet-mCherry* promoter was expressed in all cells, only a fraction of cells were positive for *PprgH-YFP* or *PfliC-eCFP*. (B and C) Flow cytometry analysis of WT *S. Typhimurium* with pZS *Ptet-mCherry PprgH-YFP Ptet-eCFP* or pZS *Ptet-mCherry PprgH-YFP PfliC-eCFP*. Cells were cultured under the same conditions as the ones described above for panel A. A significantly higher percentage of *fliC*-ON cells were *prgH*-ON than *fliC*-OFF cells. The data here are representative of results from at least four biological replicates. The *P* values were determined using the  $\chi^2$  test ( $n = \sim 10,000$ ). AU, arbitrary units. (D) Fold enrichment was calculated as the percentage of *prgH*-ON cells among *eCFP*-ON cells divided by the percentage of all *prgH*-ON cells in the whole population. The probability of *prgH*-ON among the *fliC*-ON cells is 2-fold higher than for the overall population and 4-fold higher than for the *fliC*-OFF cells. Error bars represent 1 standard deviation (SD) from the mean ( $n = 4$ ). The *P* value in panel D was determined using the unpaired *t* test.

We also found that deleting *flhDC* or *fliZ* decreased the fraction of *prgH*-ON cells (Fig. 2), supporting the cross talk between flagellar and SPI-1 pathways at the single-cell level.

Previous studies suggest that nonmotile *Salmonella* mutants are defective in host invasion (32). We confirmed that deleting *flhDC* indeed abolished the attachment of *Salmonella* to macrophage cells (Fig. 3). Interestingly, in the WT strain, *prgH*-ON/*fliC*-ON cells were substantially enriched in the subpopulation that attached to macrophages (Fig. 3), suggesting that both SPI-1 and flagellar pathways are required for effective host cell interactions.

**Flagellar expression decreases the tolerance of single *Salmonella* cells to antibiotics.** We next investigated the phenotypic variations of *fliC*-ON and *fliC*-OFF cells. We recorded the motility of single *Salmonella* cells using fluorescence and phase-contrast microscopy. While  $\sim 50\%$  of *fliC*-ON cells were highly motile, only  $<10\%$  of *fliC*-OFF cells showed motility (Fig. S2 and Video S1). In addition to *FliC*, some *Salmonella* cells also encode another flagellin, *FliB*, in phase variation (33). The small percentage of motile cells among the *fliC*-OFF cells could be due to *FliB*-dependent motility. Next, we tested the regrowth of early-stationary-phase cells and did not observe a significant difference between the *fliC*-ON and *fliC*-OFF subpopulations (Fig. S3). However, following a brief treatment (15 min) of early-stationary-phase *Salmonella* cells with the bactericidal antibiotic ciprofloxacin (Cipro) or streptomycin (Strep), a significantly higher percentage of *fliC*-OFF cells resumed multiple divisions than *fliC*-ON cells (Fig. 4, Fig. S4, and Video S2). The expression of flagellar genes is multilayered, and class 3 genes (such as *fliC*) are under the control of the sigma factor *FliA*. We further validated that similar to *fliC*-OFF cells, *fliA*-OFF cells were also more tolerant to antibiotic killing than *fliA*-ON cells (Fig. 5).

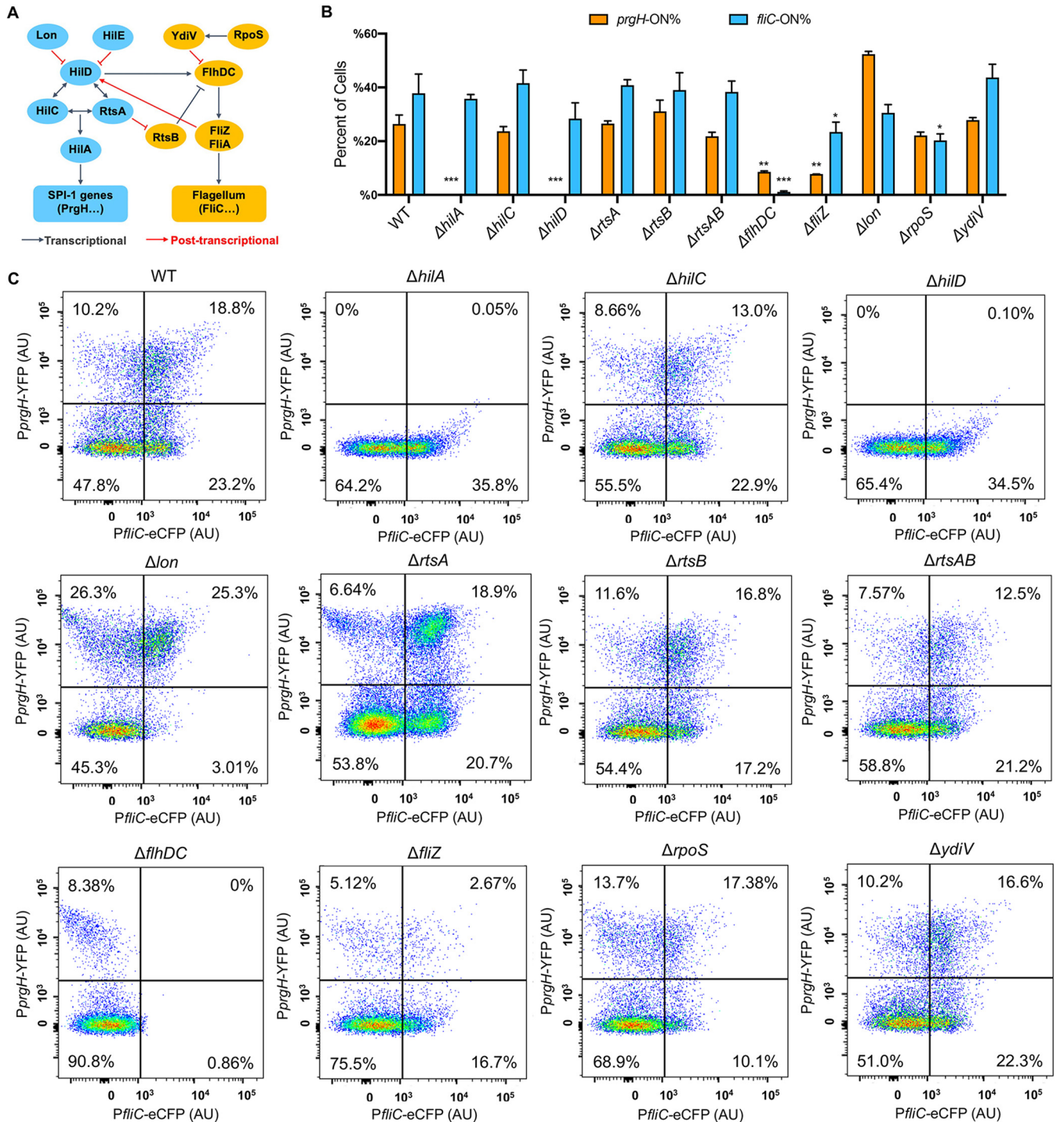


**FIG 2** Cross talk between SPI-1 and flagellar pathways in single *Salmonella* cells. (A) Scheme of cross talk between SPI-1 and flagellar genes. (B and C) Flow cytometry analysis of *prgH* and *fliC* expression in *S. Typhimurium* variants. The experimental procedure and data analysis are the same as those described in the legend of Fig. 1B. Error bars in panel B represent 1 SD from the mean ( $n = 3$ ). The  $P$  values were determined using the unpaired  $t$  test compared with the WT. \*\*,  $P < 0.01$ ; \*\*\*,  $P < 0.001$ . The results in panel C are representative of data from three biological replicates.

Early-stationary-phase *prgH*-OFF cells also appeared to survive Cipro treatment better than *prgH*-ON cells. Given the cross talk between flagellar and SPI-1 genes, we next tested which pathway was primarily responsible for the variation in antibiotic tolerance. We found that deleting *flhDC* abolished the difference in Cipro tolerance between *prgH*-ON and *prgH*-OFF cells, whereas *fliC*-OFF cells remained more tolerant than *fliC*-ON cells in the  $\Delta hilA$  strain (Fig. 4C). Deleting *flhDC* also increased the fraction

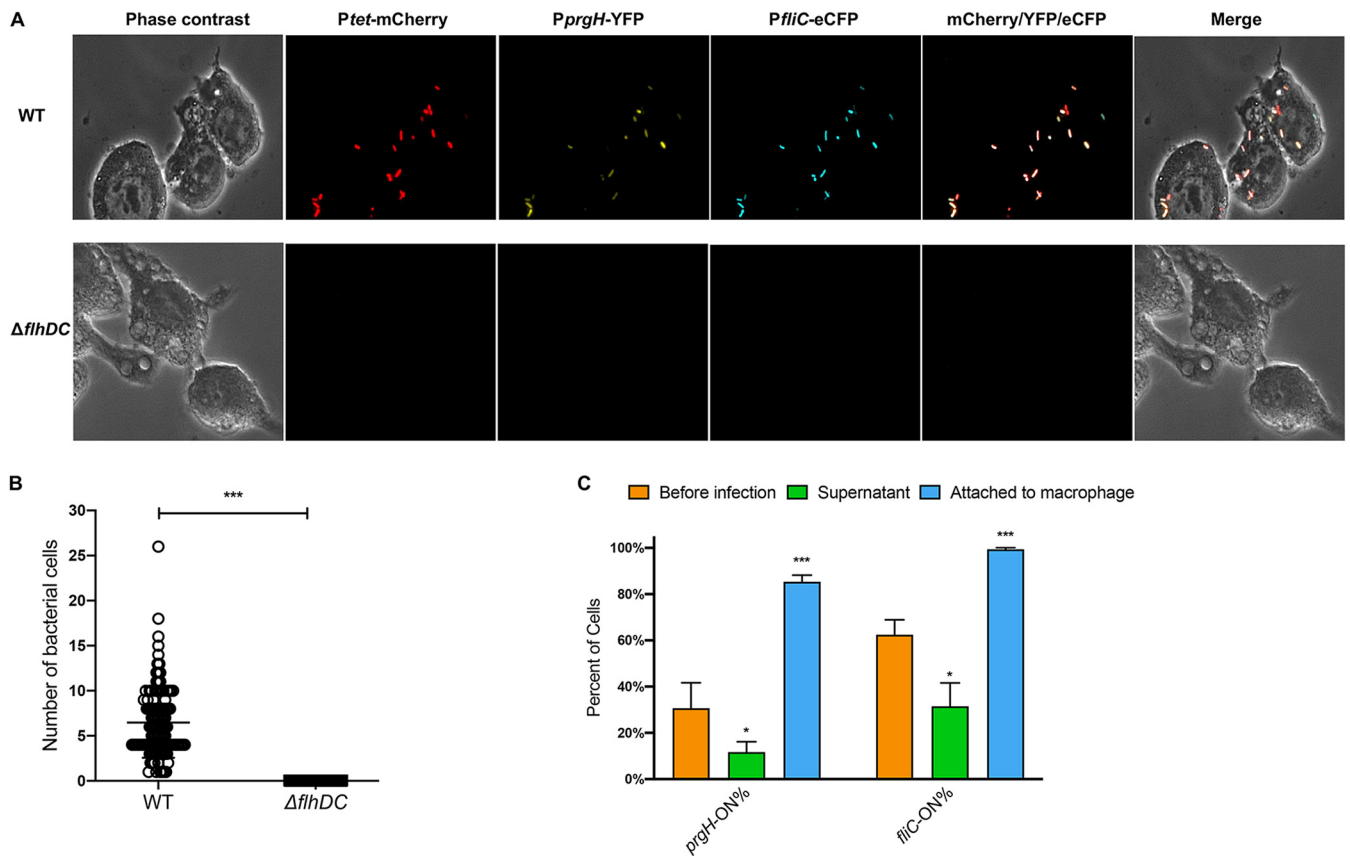


**FIG 3** SPI-1 and flagellar pathways are critical for macrophage attachment. WT and  $\Delta flhDC$  *S. Typhimurium* cells carrying pZS *Ptet*-mCherry *PprgH*-YFP *Pflic*-eCFP were grown in LB Miller at 37°C for 5 h to the early stationary phase and incubated with macrophage cells at an MOI of 50 for 15 min without centrifugation. The cultures were then washed to remove *Salmonella* cells that were not attached to macrophages. (A) Phase-contrast and fluorescence microscopy of macrophages with *Salmonella* cells. Most *Salmonella* cells attached to macrophages were *prgH*-ON and *fliC*-ON. The images are representative of results from four biological replicates. (B) Quantitation of *Salmonella* cells attached to individual macrophages. Each dot represents a macrophage cell. The data are combined from four replicates. (C) Quantitation of the percentages of *prgH*-ON and *fliC*-ON cells in the *Salmonella* populations before infection, within the supernatant postinfection, and attached to macrophages. Error bars represent 1 SD from the mean ( $n = 4$ ). The  $P$  value was determined using the unpaired  $t$  test. \*,  $P < 0.05$ ; \*\*\*,  $P < 0.001$ .

of Cipro-tolerant cells compared with the WT (Fig. S5A). Collectively, these results suggest that heterogeneous flagellar expression, instead of the SPI-1 pathway, promotes variation in transient antibiotic tolerance in *Salmonella* under the tested conditions.

**Flagella compete with efflux for PMF to decrease antibiotic tolerance.** Many Gram-negative bacteria, including *Salmonella*, exhibit robust efflux activities to remove toxic small molecules (e.g., antibiotics) from cells (34, 35). TolC is a key component for many resistance-nodulation-cell division (RND) efflux pumps, which use PMF to move antibiotics (including Cipro and Strep) across the double membrane from the cytoplasm to the exterior (34–37). We showed that deleting *tolC* or adding an efflux pump inhibitor, Phe-Arg- $\beta$ -naphthylamide (PA $\beta$ N) (38), abolished the difference between *fliC*-ON and *fliC*-OFF cells in Cipro tolerance (Fig. 6A). Using an efflux reporter dye, Nile red (39), we found that the  $\Delta flhDC$  mutant exhibited significantly higher efflux activity than the WT (Fig. 6B). In contrast, deleting *hilA* or *hilD* only modestly affected efflux (Fig. S6). This could not be explained by the expression of efflux genes, as deleting *flhDC* appeared to decrease, rather than increase, the percentage of cells with high expression levels of *tolC* (*tolC*-HIGH) or *acrAB* (*acrAB*-HIGH) (Fig. 7). In the WT, the *fliC*-ON subpopulation also displayed higher percentages of *tolC*-HIGH and *acrAB*-HIGH cells (Fig. 7). As both efflux and flagellar motility are driven by PMF, we hypothesized that there is a trade-off between efflux and flagellar expression due to the competition for PMF. Indeed, adding the PMF uncoupler carbonyl cyanide *m*-chlorophenylhydrazone (CCCP) or carbonyl cyanide *p*-trifluoromethoxyphenylhydrazone (FCCP) ablated

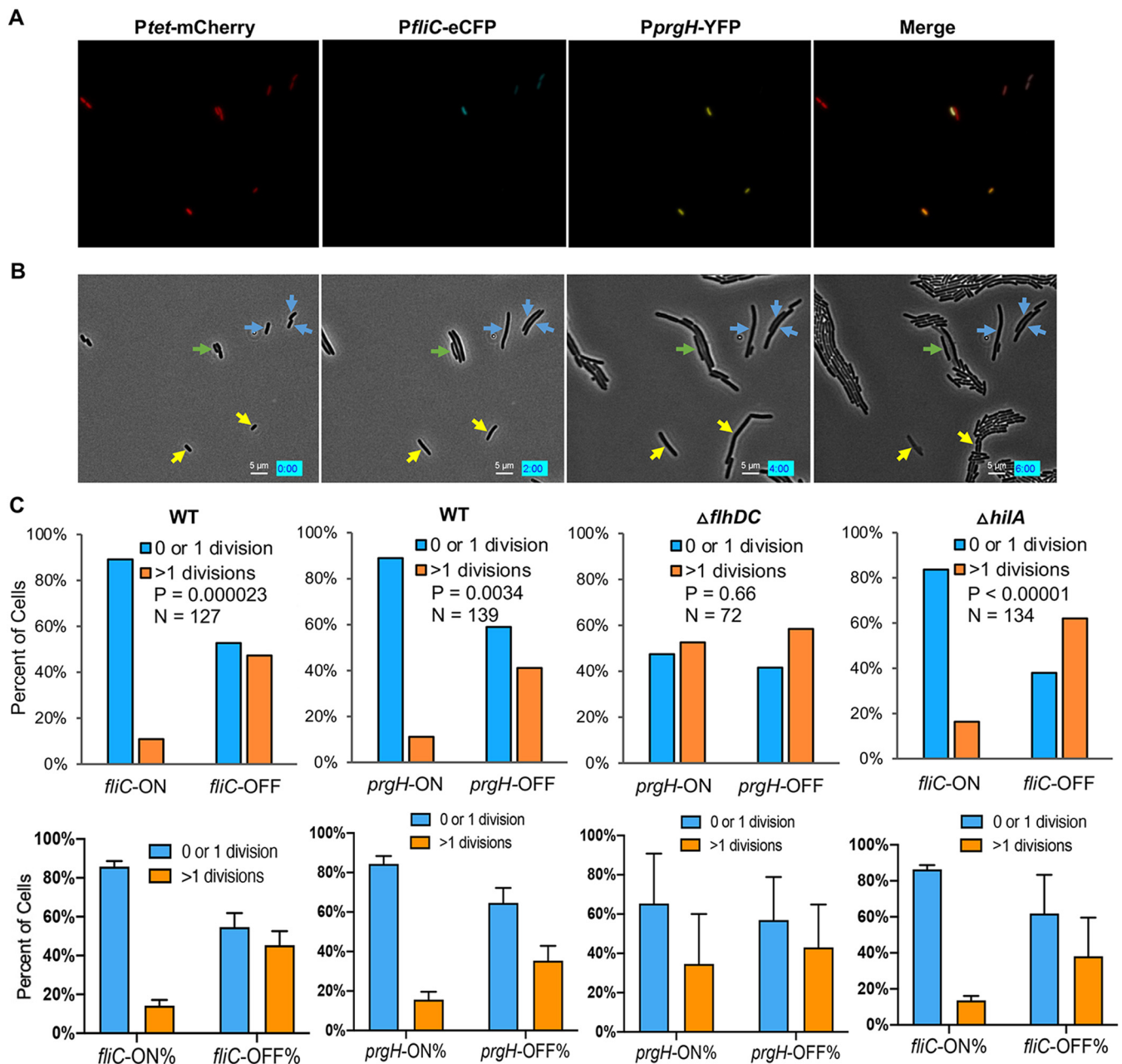


**FIG 4** Increased tolerance to Cipro in *fliC*-OFF *Salmonella* cells. (A) Fluorescence microscopy of WT *S. Typhimurium* carrying pZS *Ptet*-mCherry *PprgH*-YFP *PfliC*-eCFP. Cells were grown in LB Miller at 37°C for 5 h to the early stationary phase, treated with 0.1  $\mu$ g/ml (7 times the MIC) Cipro for 15 min, and spread onto an LB agar pad prior to microscopy. (B) Time-lapse growth of cells in panel A. Yellow, cyan, and green arrows indicate *prgH*-ON/*fliC*-OFF, *prgH*-OFF/*fliC*-ON, and *prgH*-ON/*fliC*-ON cells, respectively. The other cells are *prgH*-OFF/*fliC*-OFF. While some cells resumed multiple divisions, others underwent no division or only one division before growth arrest or cell lysis. (C) Statistics of *fliC*-ON and *fliC*-OFF cells surviving Cipro treatment in panels A and B. *fliC*-OFF cells show a significantly higher level of survival following Cipro treatment than *fliC*-ON cells in the WT and  $\Delta$ *hilA* strains. These results are representative (top) and averages (bottom) of data from at least two independent experiments. The *P* values were determined using the  $\chi^2$  test.

the difference observed between *fliC*-ON and *fliC*-OFF cells in Cipro tolerance (Fig. 8). Deleting the *motAB* genes, which encode flagellar motor proteins that drive the rotation of flagella using PMF, also abolished the difference in antibiotic tolerance between *fliC*-ON and *fliC*-OFF cells (Fig. S5B). Furthermore, we used an intracellular pH indicator, BCECF-AM [2',7'-bis-(2-carboxyethyl)-5 (and -6)-carboxyfluorescein acetoxyethyl ester], and found that in *fliC*-OFF cells, a larger percentage exhibited lower intracellular proton concentrations (higher BCECF signals and pH) than in *fliC*-ON cells (Fig. 8). The  $\Delta$ *flhDC* mutant also had a larger percentage of cells with higher BCECF signals than the

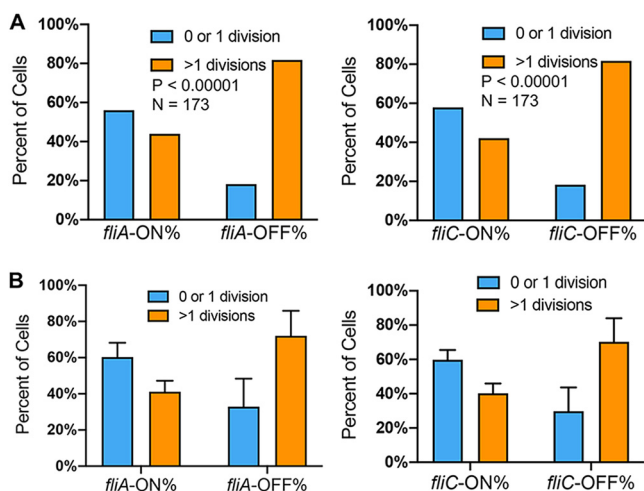


**FIG 5** Increased tolerance to Cipro in *fliA*-OFF cells. WT *S. Typhimurium* cells carrying pZS *Ptet-mCherry P*fliA*-YFP P*fliC*-eCFP* were grown and treated as described in the legend of Fig. 3. These results are representative (top) and averages (bottom) of data from three independent experiments. The *P* values were determined using the  $\chi^2$  test.

WT. As the extracellular pH remained the same for all cells, this implies that *fliC*-OFF cells have higher  $\Delta$ pH (and likely higher PMF) than *fliC*-ON cells overall. Furthermore, the addition of glucose to the media abolished the difference in Cipro tolerance between *fliC*-ON and *fliC*-OFF cells (Fig. S7), presumably due to an increase in PMF. Together, our data support that the expression of flagella costs PMF and reduces efflux efficiency, thereby decreasing tolerance to antibiotics (Fig. 9).

## DISCUSSION

Flagellar motility is a mechanism commonly used by bacteria to search for nutrients and hosts. However, the expression and assembly of flagella are also energetically costly processes (40, 41). It is remarkable that some bacteria, such as *Salmonella*, use a bet-hedging mechanism to express flagellar genes heterogeneously within a population (23, 24, 42). Our work here reveals a previously unknown benefit of the differential expression of flagellar genes. We show that *fliC*-OFF *Salmonella* cells that do not express flagella are more tolerant to antibiotics (Fig. 4; see also Fig. S4 in the supplemental material). Due to the cost of proton motive force to drive motility, flagellum-ON cells are less capable of removing intracellular antibiotics through efflux than flagellum-OFF cells (Fig. 9). It is also interesting to note that the expression of flagellar and SPI-1 genes appears to be positively correlated (Fig. 1). SPI-1 genes are essential for *Salmonella* to invade host cells (15), and nonmotile *Salmonella* mutants have been shown to exhibit a substantial decrease in host cell invasion *in vitro* and *in vivo* (32). Consistently, we show that  $\Delta$ *FlhDC* mutant cells are defective in attachment to macrophage cells (Fig. 3). At the single-cell level, macrophage-attached *Salmonella* cells are significantly enriched in *prgH*-ON and *fliC*-ON cells (Fig. 3). Coupling the expression of the SPI-1 secretion system with flagella would therefore enable *prgH*-ON/*fliC*-ON cells to quickly move toward and invade the host cells, whereas *prgH*-OFF/*fliC*-OFF cells remain in the extracellular environment, such as the intestinal lumen of mammalian hosts. The intestinal lumen is enriched in antimicrobial molecules, such as antimicrobials secreted by competing microbes as well as bile acids from the host (43, 44). Shutting off both SPI-1 and flagellar pathways would enable these *Salmonella* cells to maximize their efflux activity and remove toxic molecules, allowing survival and growth.

The cross talk between SPI-1 and flagellar pathways is complex and involves multiple factors, including FlhDC, FlhZ, RtsAB, and HilD. HilD, RtsA, and HilC form a positive

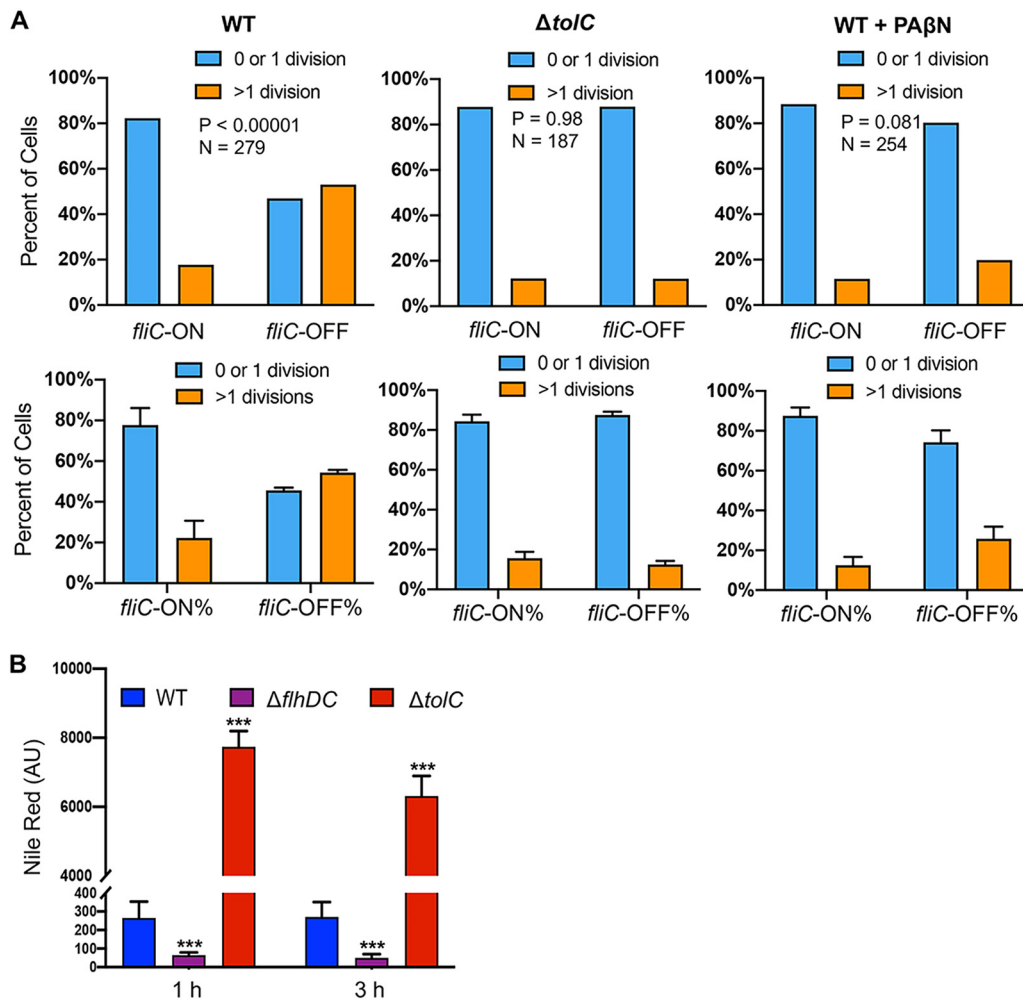


**FIG 6** Increased antibiotic tolerance in *fliC*-OFF cells depends on efflux. (A) Statistics of *fliC*-ON and *fliC*-OFF *S. Typhimurium* cells surviving Cipro (0.1  $\mu\text{g/ml}$ ) treatment as described in the legend of Fig. 3. Cells in the right panels were treated with the efflux inhibitor PA $\beta$ N (20  $\mu\text{g/ml}$ ) together with Cipro. These results are representative (top) and averages (bottom) of data from three independent experiments. The *P* values were determined using the  $\chi^2$  test. (B) *S. Typhimurium* cells grown to the early stationary phase were treated with the efflux reporter dye Nile red (48  $\mu\text{g/ml}$ ) and monitored for fluorescence using a plate reader. As expected, due to the efflux defect, the  $\Delta\textit{tolC}$  mutant accumulated more Nile red than the WT. The  $\Delta\textit{flhDC}$  mutant displayed a significantly lower Nile red signal than the WT, indicating higher efflux activity. Error bars represent 1 SD from the mean ( $n = 4$ ). The *P* value was determined using the unpaired *t* test. \*\*\*,  $P < 0.001$ .

feedforward loop to control the expression of SPI-1 genes (45). A previous study shows that overexpressing HilD activates the transcription of *flhDC* (46). Our reporter assay reveals that deleting *hilD* does not substantially decrease the fraction of *fliC*-ON cells (Fig. 2), suggesting that the native expression level of HilD under our growth conditions may not be high enough to dominate the cross talk between the two pathways. We also show that deleting *flhDC* or *fliZ* negatively impacts both the SPI-1 and flagellar pathways (Fig. 2), which is consistent with previous studies (47, 48).

The hierarchical expression of flagellar genes is regulated at multiple levels (49). The class 1 master regulator FlhDC controls the expression of class 2 genes such as *fliA*, and FlhA controls the expression of class 3 genes. *Salmonella* encodes two class 3 flagellins, FliC and FljB, and undergoes phase variation (33). Our motility assay shows that the fraction of motile cells is 7-fold higher in the *fliC*-ON group than in the *fliC*-OFF group (Fig. S2), suggesting that FliC is the prevalent form of flagellin under our tested conditions. The small percentage of motile cells among the *fliC*-OFF cells could be due to FljB-dependent motility. To test the effect of phase variation on the heterogeneity

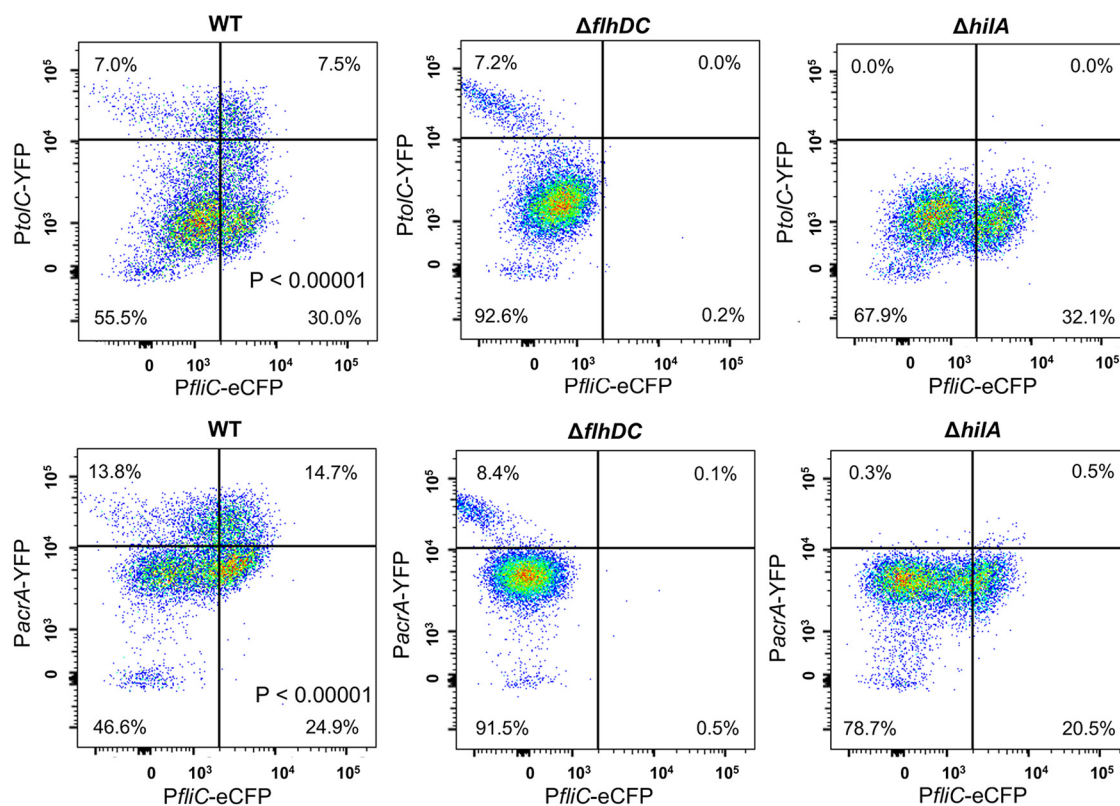


**FIG 7** Flow cytometry of *Salmonella* variants carrying flagellar and efflux reporters. *Salmonella* variants carrying pZS *Ptet-mCherry PtoIc-YFP PflIC-eCFP* or pZS *Ptet-mCherry PacrA-YFP PflIC-eCFP* were grown in LB Miller at 37°C for 5 h to the early stationary phase and analyzed by flow cytometry. AcrAB-TolC is a major multidrug efflux pump that removes Cipro and other antibiotics from *Salmonella* cells using proton motive force. Compared with *fliC*-OFF cells, *fliC*-ON cells in the WT strain exhibit high expression levels of *PtoIc* and *PacrA*. Deleting *flhDC* or *hilA* also decreases the fractions of *tolC*-HIGH and *acrA*-HIGH cells. The *P* values were determined using the  $\chi^2$  test. These results are representative of data from at least four biological replicates.

of antibiotic tolerance, we constructed a reporter using YFP under the control of *PfliA*, which is upstream of phase variation. We show that like *fliC*-ON cells, *fliA*-ON cells are also more sensitive to antibiotic killing than *fliA*-OFF cells (Fig. 5), further supporting our model of a flagellum-efflux trade-off (Fig. 9).

Antibiotic tolerance and resistance pose a severe and urgent threat to human health (6–8). A significant cause of antibiotic failure is the efflux activity in many bacterial pathogens, especially the Gram-negative bacteria (34). *Salmonella* expresses multiple efflux pumps. One major family is the TolC-dependent RND efflux pumps, which use PMF to remove many clinically important antibiotics, such as Cipro and Strep used in this study (34–37). Cipro and Strep are representatives of fluoroquinolone and aminoglycoside antibiotics that target DNA replication and protein synthesis, respectively, and Cipro is frequently used as a frontline antibiotic to treat *Salmonella* infections. We show that the differential tolerance to Cipro between *fliC*-ON and *fliC*-OFF cells depends on the presence of TolC and PMF (Fig. 5 to 7), revealing a novel mechanism of antibiotic tolerance resulting from the trade-off between flagellar motility and efflux. It is therefore advantageous for the *Salmonella* population to maintain the heterogeneous expression of flagellar genes among individual cells, which provides a bet-hedging mechanism for optimal adaptation to ever-changing environments. In addition to *Salmonella*, heterogeneous expression of flagella has been observed in some pathogenic *Escherichia coli* strains (50). Given that PMF is used to drive flagellar motility and efflux in many bacteria (35, 41), it is tempting to speculate that the trade-off between the two also occurs in other bacterial species, which needs to be investigated in future studies. Previous studies have also suggested that the heterogeneous expression of

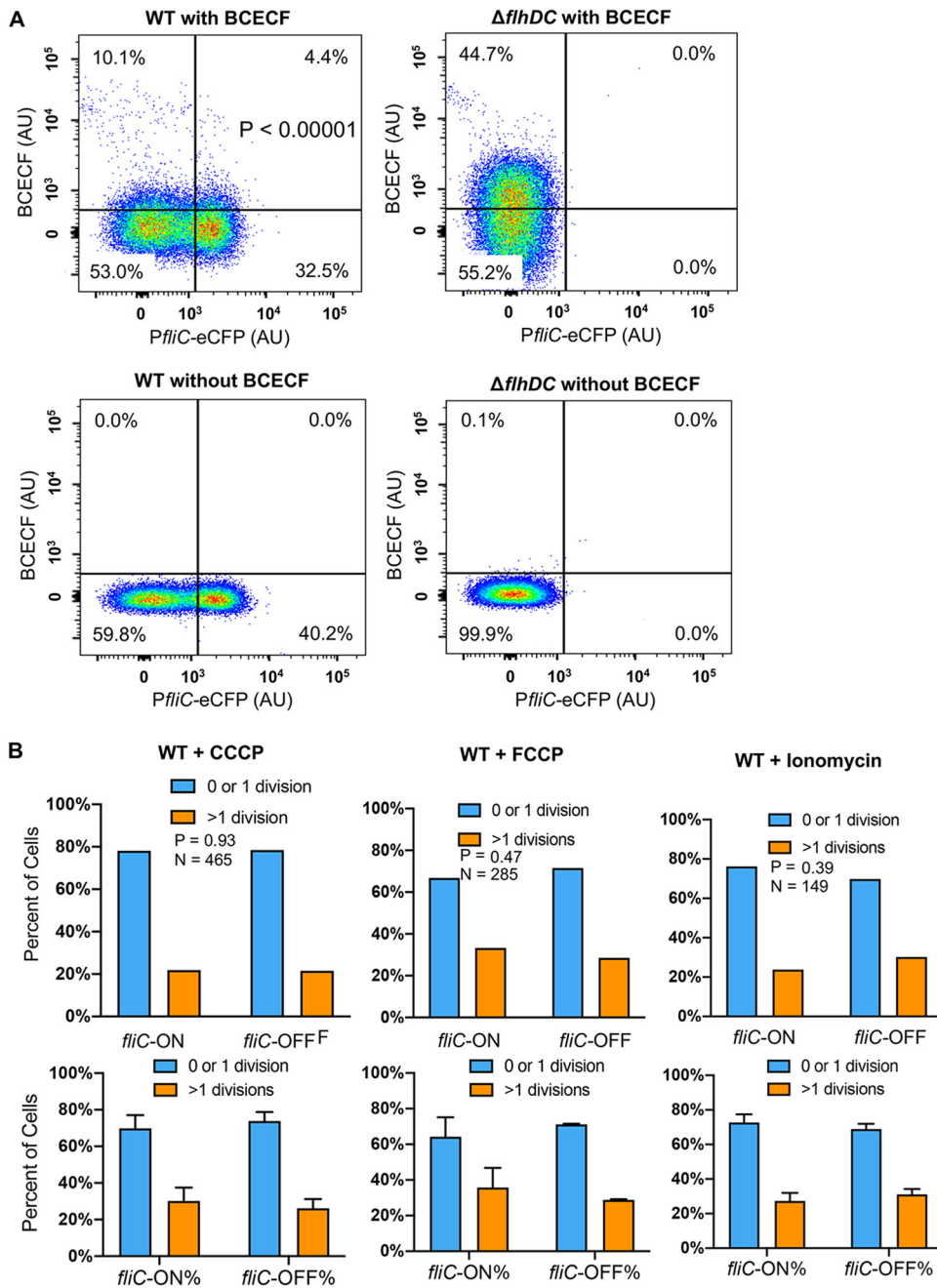


**FIG 8** Proton motive force affects differential antibiotic tolerance between *fliC*-ON and *fliC*-OFF cells. (A) WT and  $\Delta flhDC$  *Salmonella* strains carrying pZS *PflilC-eCFP* were grown to the early stationary phase, treated with the intracellular pH dye BCECF-AM (40  $\mu$ M), and analyzed using flow cytometry. A significantly higher percentage of *fliC*-OFF cells have high BCECF signals (indicating higher pH and lower intracellular protein concentrations) than *fliC*-ON cells. Deleting *flhDC* also increases the fraction of high-BCECF cells. The *P* value was determined using the  $\chi^2$  test ( $n = \sim 30,000$ ). These results are representative of data from at least three biological replicates. (B) Statistics of *fliC*-ON and *fliC*-OFF *S. Typhimurium* cells surviving Cipro (0.1  $\mu$ g/ml) treatment as described in the legend of Fig. 3. The addition of the ionophore CCCP (10  $\mu$ g/ml), FCCP (10  $\mu$ g/ml), or ionomycin (1  $\mu$ g/ml) abolished the difference in Cipro tolerance between *fliC*-ON and *fliC*-OFF cells. CCCP and FCCP are proton ionophores; ionomycin causes the efflux of cations like  $Ca^{2+}$  and the simultaneous influx of protons (54). Therefore, all three ionophores disrupt the PMF. These results are representative (top) and averages (bottom) of data from three independent experiments. The *P* values were determined using the  $\chi^2$  test.

SPI-1 cells contributes to persistence in the *Salmonella* population (51, 52). Our work here shows that the flagellar pathway, instead of SPI-1, contributes to the transient tolerance to antibiotics (Fig. 3), thus highlighting distinct mechanisms underlying antibiotic tolerance and persistence.

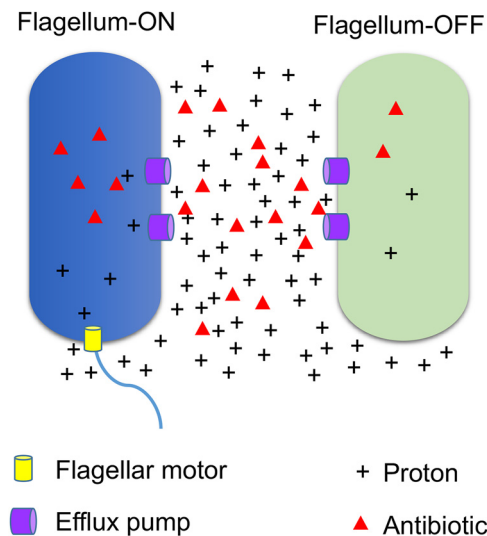


**FIG 9** Model for the trade-off between flagellar expression and efflux activity leading to antibiotic tolerance. Flagellar rotation and efflux are two of the major biological processes that use PMF as the driving force. Motile cells (flagellum-ON) consume PMF through the continuous rotation of flagella, which decreases the PMF and, therefore, the efflux activity. This leads to the accumulation of a higher level of intracellular toxic molecules, including antibiotics, in flagellum-ON cells than in flagellum-OFF cells.

## MATERIALS AND METHODS

**Bacterial strains, plasmids, and growth conditions.** All *Salmonella* strains (Table 1) used in this study are derived from *S. Typhimurium* ATCC 14028s. *Salmonella* serovar Typhimurium gene deletion mutants were constructed essentially as previously described (53). Briefly, the Flp recombination target (FRT)-flanked chloramphenicol resistance gene (*cat*) was amplified by PCR from plasmid pKD3 using primers shown in Table S1 in the supplemental material. The resulting PCR products were purified and electroporated into *S. Typhimurium* ATCC 14028s cells harboring plasmid pKD46 expressing the Red recombinase. The recombinants were selected on Luria broth (LB) plates containing chloramphenicol at 37°C and verified by PCR. All strains used in this study were cultured in LB Lennox (containing 10 g/liter of tryptone, 5 g/liter of yeast extract, and 5 g/liter of NaCl) or LB Miller (containing 10 g/liter of tryptone, 5 g/liter of yeast extract, and 10 g/liter of NaCl). The following antibiotics were used: ciprofloxacin at 0.1  $\mu\text{g/ml}$ , ampicillin at 100  $\mu\text{g/ml}$ , chloramphenicol at 25  $\mu\text{g/ml}$ , and streptomycin at 60  $\mu\text{g/ml}$ .

For the construction of the *PprgH-YFP*, *PfliA-YFP*, and *PfliC-eCFP* fusions, the promoter regions of *prgH*, *fliA*, and *fliC* containing sequences of 500 bp upstream of the start codons were amplified from strain ATCC 14028s genomic DNA by PCR. The DNA fragments were fused to plasmid pZS *Ptet-mCherry Ptet-YFP* or pZS *Ptet-eCFP* using the In-Fusion HD cloning kit according to the manufacturer's instructions.

**Time-lapse microscopy.** Cultures grown overnight in LB Lennox were diluted 1:200 in LB Miller and grown aerobically for 5 h at 37°C. All cultures were normalized to an optical density at 600 nm ( $\text{OD}_{600}$ ) of  $\sim 0.1$ , and ciprofloxacin was added to a final concentration of 0.1  $\mu\text{g/ml}$ . Following 15 min of incubation at 37°C with agitation, cultures were harvested by centrifugation and resuspended in 100  $\mu\text{l}$  LB. Two microliters of the resulting cultures was placed on a 1.5% agarose LB pad within a Gene Frame (Thermo Fisher Scientific). Fluorescence images were taken at the initial time point for quantitation. Cells were then imaged for 6 to 10 h at room temperature with a 60 $\times$  phase-contrast lens at 20-min intervals. Image analysis was performed using a BZ-X800 analyzer (Keyence).

**Efflux activity assay.** Cultures of bacteria grown overnight were diluted 1:200 into fresh LB Miller and incubated for 5 h at 37°C. All cultures were normalized to the same  $\text{OD}_{600}$ , and aliquots (100  $\mu\text{l}$ ) were transferred to 96-well plates. Nile red was added to the cells at a final concentration of 48  $\mu\text{g/ml}$ , and the cells were incubated with agitation for 3 h at 37°C. The fluorescence intensity was recorded in a Synergy H1 microplate reader (BioTek) using an excitation wavelength of 549 nm and an emission wavelength of 628 nm.

**Flow cytometry analysis.** Cultures grown overnight in LB Lennox were diluted 1:200 in LB Miller and grown aerobically for 5 h at 37°C. BCECF acetoxymethyl ester (BCECF-AM) was added to a final concentration of 40  $\mu\text{M}$ , and the cultures were incubated for 30 min at 37°C. Cells were diluted in phosphate-buffered saline (PBS) and directly measured on a BD FACSCanto II flow cytometer at a low flow rate. In all, 10,000 to 30,000 gated events were acquired for each sample. The density plots show the distribution of promoter activities in individual cells as determined based on YFP and eCFP fluorescence. Data were further analyzed using FlowJo software.

**Susceptibility to ciprofloxacin.** The MIC of ciprofloxacin was determined in 96-well microtiter plates. Mid-log-phase cultures were added to LB medium containing 2-fold serial dilutions of ciprofloxacin with a final inoculum size of  $10^5$  CFU/ml. Plates were incubated at 37°C with agitation for 18 h. The MIC was defined as the lowest concentration that completely inhibited visible growth.

**TABLE 1** List of strains and plasmids<sup>a</sup>

Strain, plasmid, chemical, peptide, recombinant protein, or assay	Source or reference	Description or origin
<b>Strains</b>		
<i>S. Typhimurium</i> ATCC 14028s (WT)	ATCC	NA
$\Delta hilA$ ( $\Delta hilA::cat$ )	This study	Region from positions 3040096–3041751 ( $\Delta 2$ –552 aa) replaced by <i>cat</i>
$\Delta hilC$ ( $\Delta hilC::cat$ )	This study	Region from positions 3032347–3033228 ( $\Delta 2$ –294 aa) replaced by <i>cat</i>
$\Delta hilD$ ( $\Delta hilD::cat$ )	Lab collection	Region from positions 3038076–3038999 ( $\Delta 2$ –308 aa) replaced by <i>cat</i>
$\Delta lon$ ( $\Delta lon::cat$ )	Lab collection	Region from positions 506238–508586 ( $\Delta 2$ –784 aa) replaced by <i>cat</i>
$\Delta rtsA$ ( $\Delta rtsA::FRT$ )	This study	Region from positions 4573934–4574584 ( $\Delta 2$ –217 aa) replaced by FRT
$\Delta rtsB$ ( $\Delta rtsB::cat$ )	This study	Region from positions 4573428–4573715 ( $\Delta 1$ –96 aa) replaced by <i>cat</i>
$\Delta rtsAB$ ( $\Delta rtsAB::cat$ )	This study	Region from positions 4573428–4574584 ( $\Delta rtsA2$ –292 aa $\Delta rtsB1$ –96 aa) replaced by <i>cat</i>
$\Delta flhDC$ ( $\Delta flhDC::cat$ )	This study	Region of positions 2032540–2033471 ( $\Delta flhD1$ –117 aa $\Delta flhC1$ –193 aa) replaced by <i>cat</i>
$\DeltafliZ$ ( $\DeltafliZ::cat$ )	Lab collection	Region from positions 2055542–2056093 ( $\Delta 2$ –183 aa) replaced by <i>cat</i>
$\Delta rpoS$ ( $\Delta rpoS::cat$ )	Lab collection	Region from positions 3085731–3086723 ( $\Delta 1$ –331 aa) replaced by <i>cat</i>
$\Delta ydiV$ ( $\Delta ydiV::cat$ )	This study	Region from positions 1432777–1433484 ( $\Delta 2$ –237 aa) replaced by <i>cat</i>
<b>Plasmids</b>		
pKD46	Lab collection	Rep101; Amp <sup>r</sup>
pKD3	Lab collection	R6K $\gamma$ ori; Amp <sup>r</sup> and Cam <sup>r</sup>
pCP20	Lab collection	Rep101(Ts); Amp <sup>r</sup> and Cam <sup>r</sup>
pZS Ptet- <i>mCherry</i> PprgH-YFP PflIC-eCFP	This study	Rep101; Amp <sup>r</sup>
pZS Ptet- <i>mCherry</i> PflIA-YFP PflIC-eCFP	This study	Rep101; Amp <sup>r</sup>
pZS PflIC-eCFP	This study	Rep101; Amp <sup>r</sup>
pZS Ptet- <i>mCherry</i> Ptet-YFP	Lab collection	Rep101; Amp <sup>r</sup>
pZS Ptet-eCFP	Lab collection	Rep101; Amp <sup>r</sup>
<b>Chemicals, peptides, and recombinant proteins</b>		
Ciprofloxacin	Acros Organics	Catalog no. 85721331
Chloramphenicol	Sigma	Catalog no. C0378
Ampicillin	Fisher Scientific	Catalog no. BP1760-5
Streptomycin	Sigma	Catalog no. S6051
CCCP	Alfa Aesar	Catalog no. L06932
FCCP	Tocris Bioscience	Catalog no. 045310
Ionomycin	Alfa Aesar	Catalog no. AAJ62448MCR
BCECF-AM	Biotium	Catalog no. 51011
Nile red	Acros Organics	Catalog no. 10658904
<b>Critical commercial assays</b>		
Taq Red master mix	Apex	Catalog no. 42138B
Q5 Hot Start high-fidelity 2 $\times$ master mix	NEB	Catalog no. M0494S
In-Fusion HD cloning plus	Takara Bio USA, Inc.	Catalog no. 638909

<sup>a</sup>NA, not applicable; aa, amino acids; NEB, New England BioLabs.

**Assay for attachment to macrophage cells.** J774A.1 (ATCC TIB-67) macrophage cells ( $\sim 10^5$  cells per well) were seeded into 96-well glass-bottom plates and left to adhere for 18 h. Infection was conducted by adding early-stationary-phase ( $\sim 5$  h) bacterial cells to each well at a multiplicity of infection (MOI) of 50. The plates were incubated at 37°C in a CO<sub>2</sub> incubator for 15 min without centrifugation. Nonadherent bacteria were then removed by three washes with PBS. The macrophage cells were fixed with 4% paraformaldehyde (PFA) for 10 min and immediately imaged with a Keyence BZ-X800 fluorescence microscope.

**Statistical analyses.** Experiments were performed using at least three biological replicates. In all cases, error bars represent the standard deviations (SD). Statistical differences were analyzed using the  $\chi^2$  test or the unpaired *t* test.

## SUPPLEMENTAL MATERIAL

Supplemental material is available online only.

**FIG S1**, PDF file, 1.6 MB.

**FIG S2**, PDF file, 0.4 MB.

**FIG S3**, PDF file, 0.5 MB.

**FIG S4**, PDF file, 0.1 MB.

**FIG S5**, PDF file, 0.2 MB.

**FIG S6**, PDF file, 0.1 MB.

**FIG S7**, PDF file, 0.2 MB.

**TABLE S1**, XLSX file, 0.01 MB.

**VIDEO S1**, MOV file, 0.4 MB.

**VIDEO S2**, MOV file, 1.1 MB.

## ACKNOWLEDGMENTS

This work was funded by NIGMS R01GM115431 and R35GM136213 to J.L.

Z.L. and J.L. designed the experiments. Z.L., A.Y., P.V., and J.L. performed the experiments. Z.L., A.Y., P.V., A.S., and J.L. analyzed the data. Z.L., A.S., and J.L. wrote the paper.

We declare no competing interests.

## REFERENCES

- Ackermann M. 2015. A functional perspective on phenotypic heterogeneity in microorganisms. *Nat Rev Microbiol* 13:497–508. <https://doi.org/10.1038/nrmicro3491>.
- Sanchez A, Golding I. 2013. Genetic determinants and cellular constraints in noisy gene expression. *Science* 342:1188–1193. <https://doi.org/10.1126/science.1242975>.
- Sampaio NMV, Dunlop MJ. 2020. Functional roles of microbial cell-to-cell heterogeneity and emerging technologies for analysis and control. *Curr Opin Microbiol* 57:87–94. <https://doi.org/10.1016/j.mib.2020.08.002>.
- Evans CR, Fan Y, Weiss K, Ling J. 2018. Errors during gene expression: single-cell heterogeneity, stress resistance, and microbe-host interactions. *mBio* 9:e01018-18. <https://doi.org/10.1128/mBio.01018-18>.
- Brauner A, Fridman O, Gefen O, Balaban NQ. 2016. Distinguishing between resistance, tolerance and persistence to antibiotic treatment. *Nat Rev Microbiol* 14:320–330. <https://doi.org/10.1038/nrmicro.2016.34>.
- Pontes MH, Groisman EA. 2020. A physiological basis for nonheritable antibiotic resistance. *mBio* 11:e00817-20. <https://doi.org/10.1128/mBio.00817-20>.
- Meylan S, Andrews IW, Collins JJ. 2018. Targeting antibiotic tolerance, pathogen by pathogen. *Cell* 172:1228–1238. <https://doi.org/10.1016/j.cell.2018.01.037>.
- Liu J, Gefen O, Ronin I, Bar-Meir M, Balaban NQ. 2020. Effect of tolerance on the evolution of antibiotic resistance under drug combinations. *Science* 367:200–204. <https://doi.org/10.1126/science.aay3041>.
- Levin-Reisman I, Ronin I, Gefen O, Braniss I, Shoshan N, Balaban NQ. 2017. Antibiotic tolerance facilitates the evolution of resistance. *Science* 355:826–830. <https://doi.org/10.1126/science.aaj2191>.
- Helaine S, Thompson JA, Watson KG, Liu M, Boyle C, Holden DW. 2010. Dynamics of intracellular bacterial replication at the single cell level. *Proc Natl Acad Sci U S A* 107:3746–3751. <https://doi.org/10.1073/pnas.1000041107>.
- Pontes MH, Groisman EA. 2019. Slow growth determines nonheritable antibiotic resistance in *Salmonella enterica*. *Sci Signal* 12:eaax3938. <https://doi.org/10.1126/scisignal.aax3938>.
- Lopatkin AJ, Stokes JM, Zheng EJ, Yang JH, Takahashi MK, You L, Collins JJ. 2019. Bacterial metabolic state more accurately predicts antibiotic lethality than growth rate. *Nat Microbiol* 4:2109–2117. <https://doi.org/10.1038/s41564-019-0536-0>.
- Gal-Mor O, Boyle EC, Grassl GA. 2014. Same species, different diseases: how and why typhoidal and non-typhoidal *Salmonella enterica* serovars differ. *Front Microbiol* 5:391. <https://doi.org/10.3389/fmicb.2014.00391>.
- GBD 2017 Non-Typhoidal Salmonella Invasive Disease Collaborators. 2019. The global burden of non-typhoidal *Salmonella* invasive disease: a systematic analysis for the Global Burden of Disease Study 2017. *Lancet Infect Dis* 19:1312–1324. [https://doi.org/10.1016/S1473-3099\(19\)30418-9](https://doi.org/10.1016/S1473-3099(19)30418-9).
- LaRock DL, Chaudhary A, Miller SI. 2015. *Salmonellae* interactions with host processes. *Nat Rev Microbiol* 13:191–205. <https://doi.org/10.1038/nrmicro3420>.
- Galan JE. 2001. *Salmonella* interactions with host cells: type III secretion at work. *Annu Rev Cell Dev Biol* 17:53–86. <https://doi.org/10.1146/annurev.cellbio.17.1.53>.
- Fabrega A, Vila J. 2013. *Salmonella enterica* serovar Typhimurium skills to succeed in the host: virulence and regulation. *Clin Microbiol Rev* 26:308–341. <https://doi.org/10.1128/CMR.00066-12>.
- Coburn B, Grassl GA, Finlay BB. 2007. *Salmonella*, the host and disease: a brief review. *Immunol Cell Biol* 85:112–118. <https://doi.org/10.1038/sj.icb.7100007>.
- Berg HC. 2003. The rotary motor of bacterial flagella. *Annu Rev Biochem* 72:19–54. <https://doi.org/10.1146/annurev.biochem.72.121801.161737>.
- Paul K, Erhardt M, Hirano T, Blair DF, Hughes KT. 2008. Energy source of flagellar type III secretion. *Nature* 451:489–492. <https://doi.org/10.1038/nature06497>.
- Stewart MK, Cummings LA, Johnson ML, Berezow AB, Cookson BT. 2011. Regulation of phenotypic heterogeneity permits *Salmonella* evasion of the host caspase-1 inflammatory response. *Proc Natl Acad Sci U S A* 108:20742–20747. <https://doi.org/10.1073/pnas.1108963108>.
- Ali SS, Soo J, Rao C, Leung AS, Ngai DH, Ensminger AW, Navarre WW. 2014. Silencing by H-NS potentiated the evolution of *Salmonella*. *PLoS Pathog* 10:e1004500. <https://doi.org/10.1371/journal.ppat.1004500>.
- Cummings LA, Wilkerson WD, Bergsbaken T, Cookson BT. 2006. In vivo, *fliC* expression by *Salmonella enterica* serovar Typhimurium is heterogeneous, regulated by ClpX, and anatomically restricted. *Mol Microbiol* 61:795–809. <https://doi.org/10.1111/j.1365-2958.2006.05271.x>.
- Stewart MK, Cookson BT. 2014. Mutually repressing repressor functions and multi-layered cellular heterogeneity regulate the bistable *Salmonella fliC* census. *Mol Microbiol* 94:1272–1284. <https://doi.org/10.1111/mmi.12828>.
- Diard M, Garcia V, Maier L, Remus-Emsermann MN, Regoes RR, Ackermann M, Hardt WD. 2013. Stabilization of cooperative virulence by the expression of an avirulent phenotype. *Nature* 494:353–356. <https://doi.org/10.1038/nature11913>.
- Sanchez-Romero MA, Casadesus J. 2021. Single cell analysis of bistable expression of pathogenicity island 1 and the flagellar regulon in *Salmonella enterica*. *Microorganisms* 9:210. <https://doi.org/10.3390/microorganisms9020210>.
- Sanchez-Romero MA, Casadesus J. 2018. Contribution of SPI-1 bistability to *Salmonella enterica* cooperative virulence: insights from single cell analysis. *Sci Rep* 8:14875. <https://doi.org/10.1038/s41598-018-33137-z>.
- Mousslim C, Hughes KT. 2014. The effect of cell growth phase on the regulatory cross-talk between flagellar and Spi1 virulence gene expression. *PLoS Pathog* 10:e1003987. <https://doi.org/10.1371/journal.ppat.1003987>.
- Fan Y, Thompson L, Lyu Z, Cameron TA, De Lay NR, Krachler AM, Ling J. 2019. Optimal translational fidelity is critical for *Salmonella* virulence and host interactions. *Nucleic Acids Res* 47:5356–5367. <https://doi.org/10.1093/nar/gkz229>.
- Eichelberg K, Galan JE. 1999. Differential regulation of *Salmonella typhimurium* type III secreted proteins by pathogenicity island 1 (SPI-1)-encoded transcriptional activators InvF and HilA. *Infect Immun* 67:4099–4105. <https://doi.org/10.1128/IAI.67.8.4099-4105.1999>.
- Smith C, Stringer AM, Mao C, Palumbo MJ, Wade JT. 2016. Mapping the regulatory network for *Salmonella enterica* serovar Typhimurium invasion. *mBio* 7:e01024-16. <https://doi.org/10.1128/mBio.01024-16>.
- Jones BD, Lee CA, Falkow S. 1992. Invasion by *Salmonella typhimurium* is affected by the direction of flagellar rotation. *Infect Immun* 60:2475–2480. <https://doi.org/10.1128/iai.60.6.2475-2480.1992>.
- Bonifield HR, Hughes KT. 2003. Flagellar phase variation in *Salmonella enterica* is mediated by a posttranscriptional control mechanism. *J Bacteriol* 185:3567–3574. <https://doi.org/10.1128/JB.185.12.3567-3574.2003>.

34. Masi M, Refregiers M, Pos KM, Pages JM. 2017. Mechanisms of envelope permeability and antibiotic influx and efflux in Gram-negative bacteria. *Nat Microbiol* 2:17001. <https://doi.org/10.1038/nmicrobiol.2017.1>.
35. Du D, Wang-Kan X, Neuberger A, van Veen HW, Pos KM, Piddock LJV, Luisi BF. 2018. Multidrug efflux pumps: structure, function and regulation. *Nat Rev Microbiol* 16:523–539. <https://doi.org/10.1038/s41579-018-0048-6>.
36. Ramaswamy VK, Vargiu AV, Mallocci G, Dreier J, Ruggerone P. 2017. Molecular rationale behind the differential substrate specificity of bacterial RND multi-drug transporters. *Sci Rep* 7:8075. <https://doi.org/10.1038/s41598-017-08747-8>.
37. Rosenberg EY, Ma D, Nikaido H. 2000. AcrD of *Escherichia coli* is an aminoglycoside efflux pump. *J Bacteriol* 182:1754–1756. <https://doi.org/10.1128/JB.182.6.1754-1756.2000>.
38. Sanchez-Romero MA, Casadesus J. 2014. Contribution of phenotypic heterogeneity to adaptive antibiotic resistance. *Proc Natl Acad Sci U S A* 111:355–360. <https://doi.org/10.1073/pnas.1316084111>.
39. Whittle EE, Legood SW, Alav I, Dulyayangkul P, Overton TW, Blair JMA. 2019. Flow cytometric analysis of efflux by dye accumulation. *Front Microbiol* 10:2319. <https://doi.org/10.3389/fmicb.2019.02319>.
40. Subramanian S, Kearns DB. 2019. Functional regulators of bacterial flagella. *Annu Rev Microbiol* 73:225–246. <https://doi.org/10.1146/annurev-micro-020518-115725>.
41. Chevance FF, Hughes KT. 2008. Coordinating assembly of a bacterial macromolecular machine. *Nat Rev Microbiol* 6:455–465. <https://doi.org/10.1038/nrmicro1887>.
42. Wang X, Koirala S, Aldridge PD, Rao CV. 2020. Two tandem mechanisms control bimodal expression of the flagellar genes in *Salmonella enterica*. *J Bacteriol* 202:e00787-19. <https://doi.org/10.1128/JB.00787-19>.
43. Garcia-Gutierrez E, Mayer MJ, Cotter PD, Narbad A. 2019. Gut microbiota as a source of novel antimicrobials. *Gut Microbes* 10:1–21. <https://doi.org/10.1080/19490976.2018.1455790>.
44. Voronova V, Sokolov V, Al-Khaifi A, Straniero S, Kumar C, Peskov K, Helmlinger G, Rudling M, Angelin B. 2020. A physiology-based model of bile acid distribution and metabolism under healthy and pathologic conditions in human beings. *Cell Mol Gastroenterol Hepatol* 10:149–170. <https://doi.org/10.1016/j.jcmgh.2020.02.005>.
45. Saini S, Ellermeier JR, Slauch JM, Rao CV. 2010. The role of coupled positive feedback in the expression of the SPI1 type three secretion system in *Salmonella*. *PLoS Pathog* 6:e1001025. <https://doi.org/10.1371/journal.ppat.1001025>.
46. Singer HM, Kuhne C, Deditius JA, Hughes KT, Erhardt M. 2014. The *Salmonella* Spi1 virulence regulatory protein HlID directly activates transcription of the flagellar master operon *flhDC*. *J Bacteriol* 196:1448–1457. <https://doi.org/10.1128/JB.01438-13>.
47. Chubiz JE, Golubeva YA, Lin D, Miller LD, Slauch JM. 2010. FlhZ regulates expression of the *Salmonella* pathogenicity island 1 invasion locus by controlling HlID protein activity in *Salmonella enterica* serovar Typhimurium. *J Bacteriol* 192:6261–6270. <https://doi.org/10.1128/JB.00635-10>.
48. Saini S, Slauch JM, Aldridge PD, Rao CV. 2010. Role of cross talk in regulating the dynamic expression of the flagellar *Salmonella* pathogenicity island 1 and type 1 fimbrial genes. *J Bacteriol* 192:5767–5777. <https://doi.org/10.1128/JB.00624-10>.
49. Chilcott GS, Hughes KT. 2000. Coupling of flagellar gene expression to flagellar assembly in *Salmonella enterica* serovar Typhimurium and *Escherichia coli*. *Microbiol Mol Biol Rev* 64:694–708. <https://doi.org/10.1128/MMBR.64.4.694-708.2000>.
50. Laganenka L, Lopez ME, Colin R, Sourjik V. 2020. Flagellum-mediated mechanosensing and RflP control motility state of pathogenic *Escherichia coli*. *mBio* 11:e02269-19. <https://doi.org/10.1128/mBio.02269-19>.
51. Bakkeren E, Huisman JS, Fattinger SA, Hausmann A, Furter M, Egli A, Slack E, Sellin ME, Bonhoeffer S, Regoes RR, Diard M, Hardt WD. 2019. *Salmonella* persisters promote the spread of antibiotic resistance plasmids in the gut. *Nature* 573:276–280. <https://doi.org/10.1038/s41586-019-1521-8>.
52. Arnoldini M, Vizcarra IA, Pena-Miller R, Stocker N, Diard M, Vogel V, Beardmore RE, Hardt WD, Ackermann M. 2014. Bistable expression of virulence genes in *Salmonella* leads to the formation of an antibiotic-tolerant subpopulation. *PLoS Biol* 12:e1001928. <https://doi.org/10.1371/journal.pbio.1001928>.
53. Datsenko KA, Wanner BL. 2000. One-step inactivation of chromosomal genes in *Escherichia coli* K-12 using PCR products. *Proc Natl Acad Sci U S A* 97:6640–6645. <https://doi.org/10.1073/pnas.120163297>.
54. Kauffman RF, Taylor RW, Pfeiffer DR. 1980. Cation transport and specificity of ionomycin. Comparison with ionophore A23187 in rat liver mitochondria. *J Biol Chem* 255:2735–2739.